LETTERS
PUBLISHED ONLINE: 14 APRIL 2013 | DOI: 10.1038/NCLIMATE1864
nature climate change

Multiple greenhouse-gas feedbacks from the land biosphere under future climate change scenarios

Benjamin D. Stocker[1,2]*, Raphael Roth[1,2], Fortunat Joos[1,2], Renato Spahni[1,2], Marco Steinacher[1,2], Soenke Zaehle[3], Lex Bouwman[4,5], Xu-Ri[6] and Iain Colin Prentice[7,8]

Atmospheric concentrations of the three important greenhouse gases (GHGs) CO_2, CH_4 and N_2O are mediated by processes in the terrestrial biosphere that are sensitive to climate and CO_2. This leads to feedbacks between climate and land and has contributed to the sharp rise in atmospheric GHG concentrations since pre-industrial times. Here, we apply a process-based model to reproduce the historical atmospheric N_2O and CH_4 budgets within their uncertainties and apply future scenarios for climate, land-use change and reactive nitrogen (Nr) inputs to investigate future GHG emissions and their feedbacks with climate in a consistent and comprehensive framework[1]. Results suggest that in a business-as-usual scenario, terrestrial N_2O and CH_4 emissions increase by 80 and 45%, respectively, and the land becomes a net source of C by AD 2100. N_2O and CH_4 feedbacks imply an additional warming of 0.4–0.5 °C by AD 2300; on top of 0.8–1.0 °C caused by terrestrial carbon cycle and Albedo feedbacks. The land biosphere represents an increasingly positive feedback to anthropogenic climate change and amplifies equilibrium climate sensitivity by 22–27%. Strong mitigation limits the increase of terrestrial GHG emissions and prevents the land biosphere from acting as an increasingly strong amplifier to anthropogenic climate change.

At present, the terrestrial biosphere is mitigating anthropogenic climate change by acting as a carbon (C) sink, compensating about 30% of global CO_2 emissions from fossil and land-use sources[2]. In contrast, 44–73% of global nitrous oxide (N_2O) emissions[3,4] and 24–43% of global methane (CH_4) emissions[5], both potent GHGs, originate from land ecosystems and partly offset the cooling effect of C uptake by the land. Terrestrial N_2O and CH_4 emissions, henceforth termed eN_2O and eCH_4, are enhanced in a warm climate[6,7] and under high atmospheric CO_2 concentrations (cCO_2; ref. 8). The associated feedback loop amplifies anthropogenic climate change and is reflected in palaeo records on glacial–interglacial and centennial timescales[9,10]. However, despite its potential importance[6] there is yet a lack of studies investigating combined multiple GHG feedbacks between terrestrial ecosystems and climate.

The strength of feedbacks between land and climate is determined by the sensitivity of the forcing agents (here: eN_2O; eCH_4; terrestrial C storage, ΔC; and Albedo change) to the drivers (climate and cCO_2), and the radiative efficiency of the respective forcing agent. Earlier quantifications of terrestrial GHG feedbacks have relied on observational data and land-only models to derive the sensitivities, multiplied by the radiative efficiency[6,7,9–11]. Here, we assess multiple feedbacks from terrestrial ecosystems in a coupled Earth system model of intermediate complexity and follow a quantification framework commonly applied to measure the strength of physical climate feedbacks[1,12] (Fig. 1 and Methods). Applying future scenarios of N-deposition and N-fertilizer application in agriculture allows us to assess their impact on eN_2O and related feedbacks.

We start the discussion by exploring to which extent a process-based land biosphere model is able to reproduce the observation-based evolution of atmospheric N_2O and CH_4 concentrations (cN_2O, cCH_4) over the industrial period. Addressing the historical atmospheric GHG budgets serves as a test for the sensitivity of simulated GHG emissions to the combination of climate, cCO_2 and external forcings. LPX-Bern[13–18] is applied here to simulate the coupled cycling of carbon and nitrogen and the emissions of GHGs from agricultural and natural land and from peat. Site-scale evaluations of this model have been presented earlier[7,15–20]. For this test, we force LPX-Bern with observational data for climate[21], cCO_2 (ref. 22), Nr (N deposition[23] plus mineral N fertilizer inputs[24]) and anthropogenic land-use area change and combine simulated emissions with independent emission data from remaining sources to assess atmospheric budgets (see Methods and Supplementary Fig. S1).

For eN_2O, we confirm earlier results[24] showing that the simulated emission increase in the second half of the twentieth century matches measured concentrations (Fig. 2a). Experiments with incomplete driving factors perform worse at reproducing the observed rate of increase in the past four decades. The increase in atmospheric N_2O before AD 1920 is not captured, although an increasing manure source is prescribed. Climatic changes after the late-nineteenth-century temperature minimum are a potential driver not represented in the applied CRU climate forcing data[21].

The twentieth-century increase in cCH_4 is dominated by changes in prescribed sources (see Methods). Simulated changes in eCH_4 from boreal peatlands, inundated areas (natural and anthropogenic) and wet mineral soils remain comparably small over the industrial period. The magnitudes of these fluxes were scaled individually to match results of an atmospheric CH_4 transport inversion[19]. The small model response to twentieth-century climatic variations is consistent with the measured

[1]Climate and Environmental Physics, Physics Institute, University of Bern, 3012 Bern, Switzerland, [2]Oeschger Center for Climate Change Research, University of Bern, 3012 Bern, Switzerland, [3]Max Planck Institute for Biogeochemistry, Department for Biogeochemical Systems, 07745 Jena, Germany, [4]Department of Earth Sciences, Geochemistry, Faculty of Geosciences, Utrecht University, 3508 TA Utrecht, The Netherlands, [5]PBL Netherlands Environmental Assessment Agency, PO Box 303, 3720 AH Bilthoven, The Netherlands, [6]Laboratory of Tibetan Environment Changes and Land Surface Processes, Institute of Tibetan Plateau Research, Chinese Academy of Sciences, Beijing 100101, China, [7]Department of Biological Sciences, Macquarie University, North Ryde, New South Wales 2109, Australia, [8]Grantham Institute for Climate Change and Division of Ecology and Evolution, Imperial College, Silwood Park, Ascot SL5 7PY, UK. *e-mail: beni@climate.unibe.ch

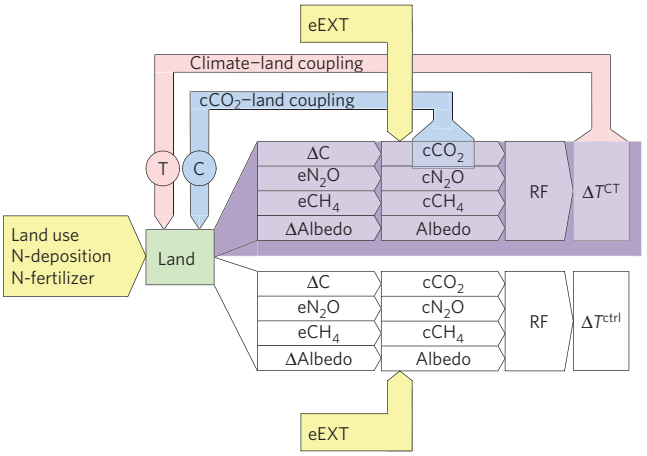

Figure 1 | Schematic of feedback loops and model set-up. Representing the fully coupled (purple background, superscript CT) and the control (uncoupled, white background, superscript ctrl) simulations. The evolution of land-use area and reactive nitrogen addition (N-deposition and N-fertilizer) is a prescribed input to the land model and the evolution of non-land biosphere-related, external emissions (eEXT) of N_2O, CO_2, CH_4 and other forcing agents (aerosols, precursors, CFCs, SF_6 and so on) is a prescribed input to the atmosphere module in both the coupled and uncoupled set-up as indicated by the yellow panels. The land model (green) simulates changes in land carbon stocks (ΔC) and the related net land-to-atmosphere CO_2 flux, terrestrial emissions of N_2O and CH_4 (eN_2O, eCH_4) and land surface Albedo changes (ΔAlbedo). These simulated changes, in combination with eEXT, yield the simulated atmospheric concentrations (cCO_2, cN_2O, cCH_4) and the surface Albedo, cause a radiative forcing (RF) and affect climate, here represented by the global mean temperature (ΔT), which scales spatial climate change anomaly patterns in Bern3D-LPX. Note that the prescribed emissions of reactive gases (CO, VOC, NO_x) affect cCH_4. Note also that even in the control set-up (ctrl), land use and Nr affect terrestrial GHG emissions, and eEXT is added and ΔT^{ctrl} is not zero. In the fully coupled set-up (CT), changes in the drivers, climate and cCO_2 relative to their pre-industrial state are communicated to the land model, whereas the land model sees none of these changes in the control set-up. In cCO_2–land coupled (C) and climate–land coupled (T) simulations only changes in one driver are communicated to the land model (see Supplementary Fig. S16). Results shown in Figs 4 and 5 are obtained by the set-up of the Bern3D-LPX model shown in here. In offline simulations for which results are shown in Figs 2 and 3, cCO_2 and climate change are not simulated, but prescribed (see Supplementary Fig. S17).

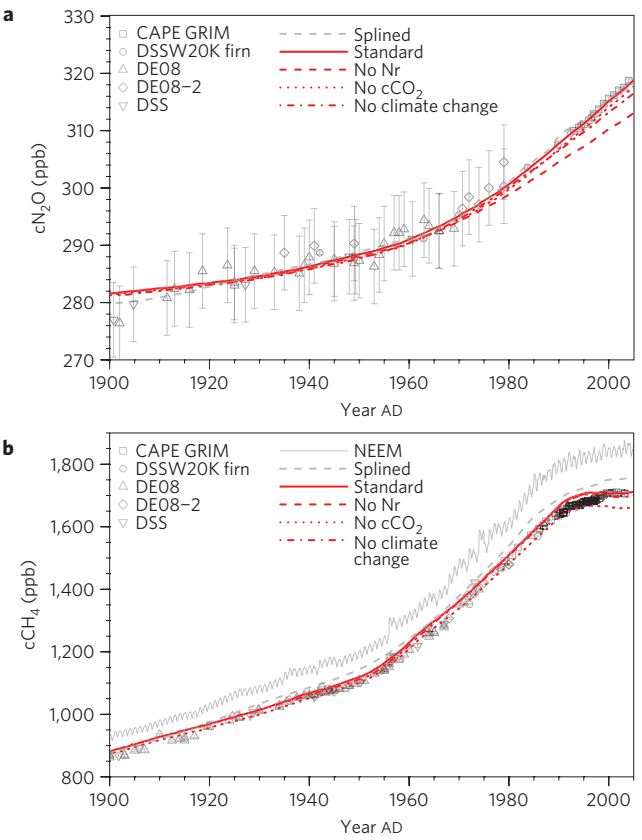

Figure 2 | Simulated and observed concentrations. a,**b**, Observed and simulated cN_2O (**a**) and cCH_4 (**b**). Observational N_2O data (grey) is from refs 22,33. Measurement precision ($\pm 1\sigma$) is given by vertical bars. The dashed grey line is a 200-yr cutoff spline through observational data. Observational CH_4 point data (grey) are from ref. 22 and represent Southern Hemispheric concentrations. The solid grey line (NEEM) is derived from Northern Hemispheric firn air data and includes seasonal variability[34]. The dashed grey line is a spline of observational Southern Hemisphere data. Simulation results (red) are from offline experiments where changes in climate, cCO_2 and Nr inputs are prescribed (standard), or where climate is held at pre-industrial levels (no climate change), cCO_2 is held constant at pre-industrial levels (no cCO_2) or Nr is held at pre-industrial levels (no Nr, see Supplementary Table S2). An oceanic N_2O source (3.3 Tg $N_2O-N\,yr^{-1}$) and a constant geological CH_4 source (38 Tg $CH_4\,yr^{-1}$), tuned to match RCP data in year AD 1900, are included.

atmospheric CH_4 record, but the small signal prevents any firm evaluation of the modelled sensitivity of eCH_4 to climate change (Fig. 2b). In conclusion, the model produces realistic global results for eN_2O and eCH_4 under plausible forcing.

Next, we assess the sensitivity of terrestrial GHG emissions to future climate, cCO_2, Nr and their combination for a stringent climate mitigation scenario that maintains the possibility of reaching the two-degree target (Representative Concentration Pathway (RCP) 2.6; ref. 25) and a high-emission/business-as-usual scenario (RCP8.5; ref. 26). Scenarios for land use, N-fertilizer and N-deposition each consistently follow socio-economic developments in the respective RCP (model inputs described in Supplementary Section S2). Climate is prescribed for each RCP using Climate Model Intercomparison Project 5 (CMIP5) output from ensemble simulations of five comprehensive climate models. This allows us to assess the influence of uncertainties in the climate evolution and in the scenario choice. Prescribed cCO_2, global temperatures and Nr inputs stabilize in RCP2.6, whereas in RCP8.5, they increase throughout the twenty-first century.

The combination and interactions of global warming, cCO_2 and external forcings (land-use change and anthropogenic Nr inputs) drive eN_2O up from a preindustrial level of 6.9 to 9.0 Tg N_2O–$N\,yr^{-1}$ by today and to 9.8–11.1 (RCP2.6) and 14.2–17.0 Tg N_2O–$N\,yr^{-1}$ by AD 2100 (RCP8.5, Fig. 3a). In RCP8.5, only 14–21% of this increase is due to external forcings alone (Fig. 3a, right panel, 'ctrl' stripe) Climate change and rising cCO_2 are responsible for the remaining amplification. Without Nr inputs, the amplification is reduced by 24–32% (Fig. 3a, right panel, empty bars).

eN_2O is governed by denitrification of reactive N in the soil, not taken up by the plant. Given sufficient nutrient availability, high cCO_2 tends to increase plant productivity, which ultimately feeds litter and soil decomposition. Warmer soil temperatures accelerate decomposition, making nutrients available for plant uptake but also increasing substrate availability for denitrification and eN_2O. Increased loads of reactive nitrogen from atmospheric deposition and on fertilized agricultural land are prone to temperature-driven denitrification, leaching to water streams and loss as N_2O. In our RCP8.5 simulations, the fraction of Nr inputs to

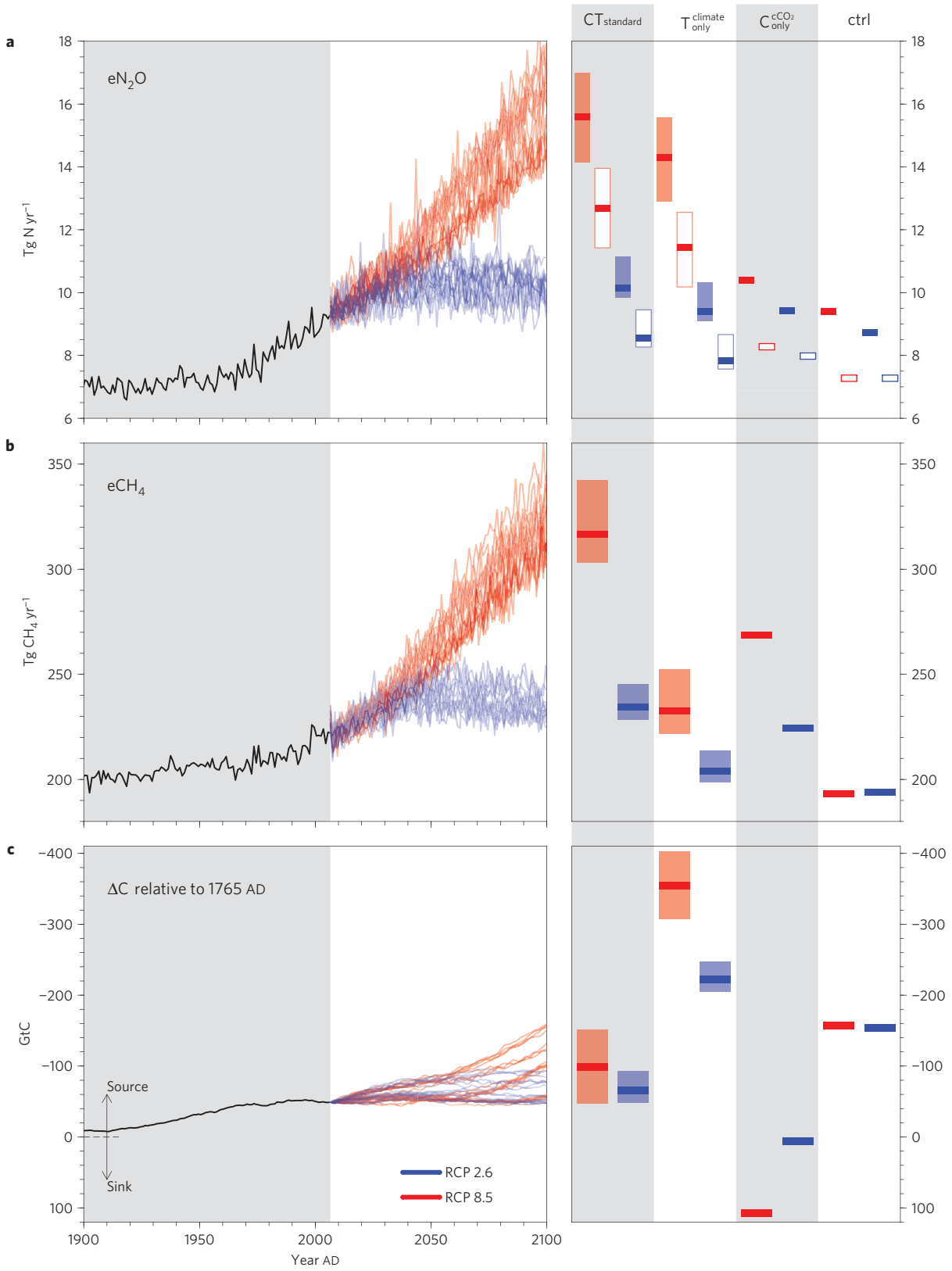

Figure 3 | Future emissions. a–c, N_2O emissions from terrestrial ecosystems and from leached N in water streams (**a**), terrestrial CH_4 emissions (**b**), and change in terrestrial C storage since AD 1765 (**c**; including land-use change) for the historical period (black), and the twenty-first century for RCP2.6 (blue) and RCP8.5 (red). Minimum, mean and maximum at the end of the twenty-first century (mean over AD 2090–2100) for emissions and C storage change for different set-ups are given by the bars in the right panel. Empty bars represent ranges of N_2O emissions in simulations with Nr inputs held at pre-industrial levels. Effects of Nr inputs on CH_4 emissions and ΔC are negligible and are thus not shown. The spread of emissions arises from different prescribed patterns of future climate change from different CMIP5 climate models. Results are from offline simulations.

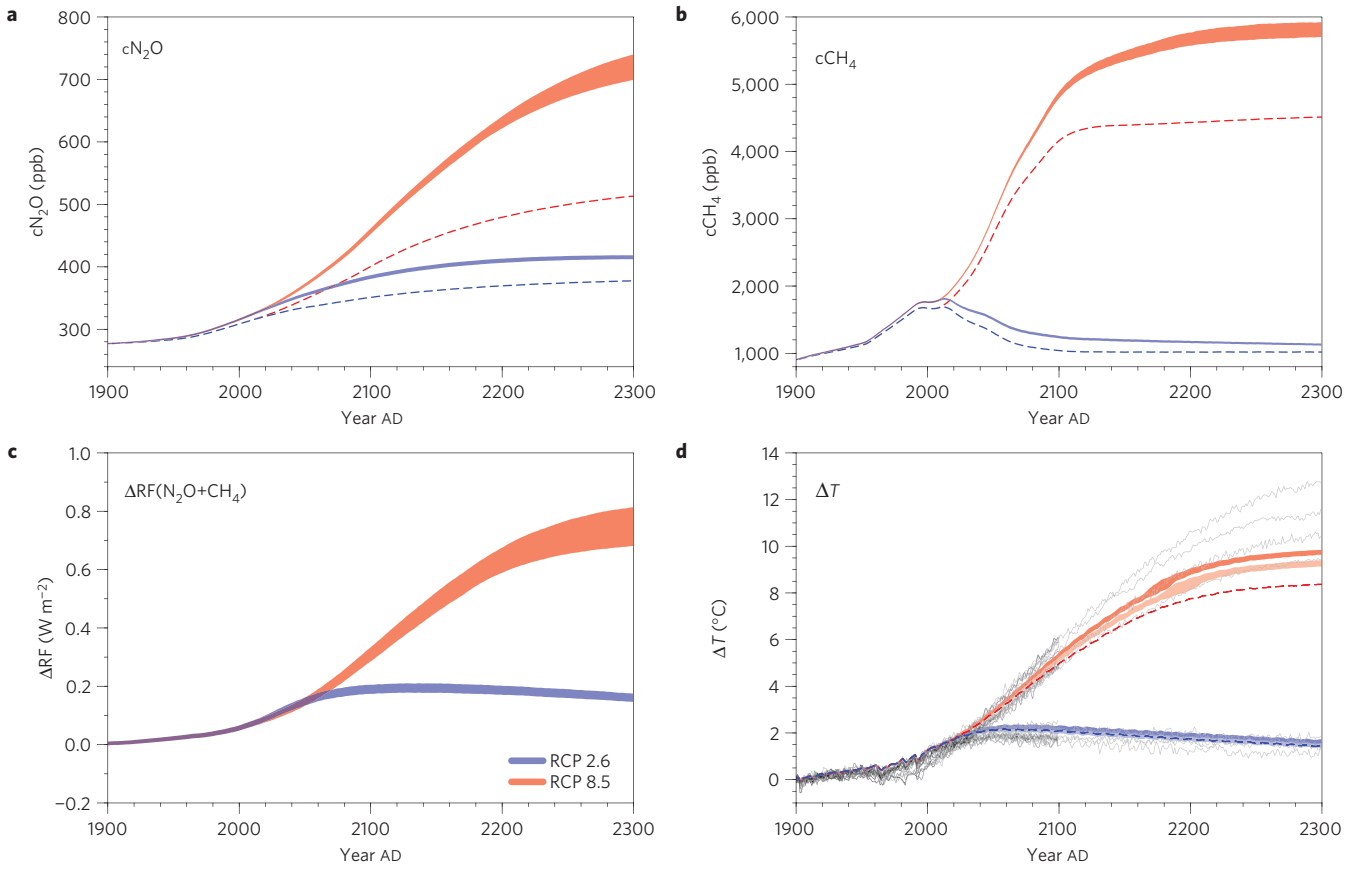

Figure 4 | Future concentrations, radiative forcing and global mean temperature. a,**b**, Simulated cN_2O (**a**) and cCH_4 (**b**) in the fully coupled (ranges) and the control (dashed lines) simulations for RCP2.6 (blue) and RCP8.5 (red). Results are from online simulations. Higher concentrations in the fully coupled simulations are due to amplified emissions in response to changes in both climate and cCO_2. **c**, Additional radiative forcing due the higher cN_2O and cCH_4 in the fully coupled simulation compared with the control simulation. Changes in cCH_4concentrations affect stratospheric cH_2O and cO_3. Resulting radiative forcings are included in RF(CH_4). **d**, Global mean temperature change in the control simulation (dashed line), the fully coupled simulation (upper range), and the fully coupled simulation without changes in eN_2O and eCH_4 affecting climate (lower, pale-coloured range) for RCP2.6 (blue) and RCP8.5 (red). Grey lines represent ΔT as simulated by the ensemble of CMIP5 models applied.

agricultural soil lost as N_2O is enhanced by 43–78% by AD 2100 owing to the interaction of Nr inputs with climate change and cCO_2 (see Supplementary Fig. S13). Such effects thus impede the application of Intergovernmental Panel on Climate Change (IPCC) N_2O emission factors to derive anthropogenic N_2O emissions from Nr inputs[27].

eCH_4 rises from 221 Tg CH_4 yr^{-1} at present to 228–245 in RCP2.6 and to 303–343 Tg CH_4 yr^{-1} in RCP8.5. eCH_4 is modelled as a fraction of soil C decomposition under anaerobic soil conditions in mineral soils and is explicitly simulated with production, oxidation and vertical transport in peatlands[17,18]. High cCO_2 ultimately enhances decomposition and affects soil moisture through water-use efficiency. It is thus the main driver of the eCH_4 increase in RCP8.5 (Fig. 2b and Supplementary Information). eCH_4 from boreal peatlands experiences the strongest increase in RCP8.5 (+120–200%). However, climate change at high northern latitudes is subject to substantial uncertainties as evidenced by the spread in CMIP5 model results. This also implies a wide range of simulated ΔC, with climate from models featuring a strong polar warming amplification yielding the largest C losses. Decline in seasonal snow cover and vegetation shifts in response to a warmer climate entail effects on surface Albedo mostly causing an further positive feedback (see Supplementary Fig. S15).

To capture the entire feedback loops between climate and land (Fig. 1), we apply the Bern3D-LPX Earth system model of intermediate complexity[28,29]. The model is forced by anthropogenic emissions, land-use change and Nr inputs. Atmospheric GHG concentrations, radiative forcing, climate change and GHG release from land ecosystems are simulated and evolve interactively.

The response of eN_2O and eCH_4 to climate and cCO_2 adds to direct anthropogenic emissions and further amplifies atmospheric concentrations. The associated additional radiative forcing (ΔRF) amplifies the temperature increase by 0.4–0.5 °C by AD 2300 in RCP8.5 (Fig. 4). ΔRF broadly scales with ΔT and is thus smaller in RCP2.6. The proportionality between ΔT and ΔRF represents the strength of the feedback and is captured by the feedback factor r (see Supplementary Equation S6).

Applying a comprehensive set of simulations following the emission pathways associated with RCP8.5 and RCP2.6 and using a formalism commonly applied to physical climate feedbacks, we quantify individual feedback factors for each forcing agent mediated by the land model and for each driver of the land response (Fig. 5).

The total land climate feedback is 0.11–0.16 (0.22–0.24) $W m^{-2} K^{-1}$ in 2100 (2300) AD and thus about an order of magnitude smaller than other physical climate feedbacks. The negative feedback arising from cCO_2 effects on ΔC (CO_2-fertilization) dominates at present but declines thereafter owing to eco-physiological saturation (see Supplementary Fig. S9) and the declining radiative efficiency of cCO_2 under high concentrations. In the long term, this negative feedback is largely compensated by the positive feedback from a warmer climate ($r^{T}_{\Delta C}$), and thus the

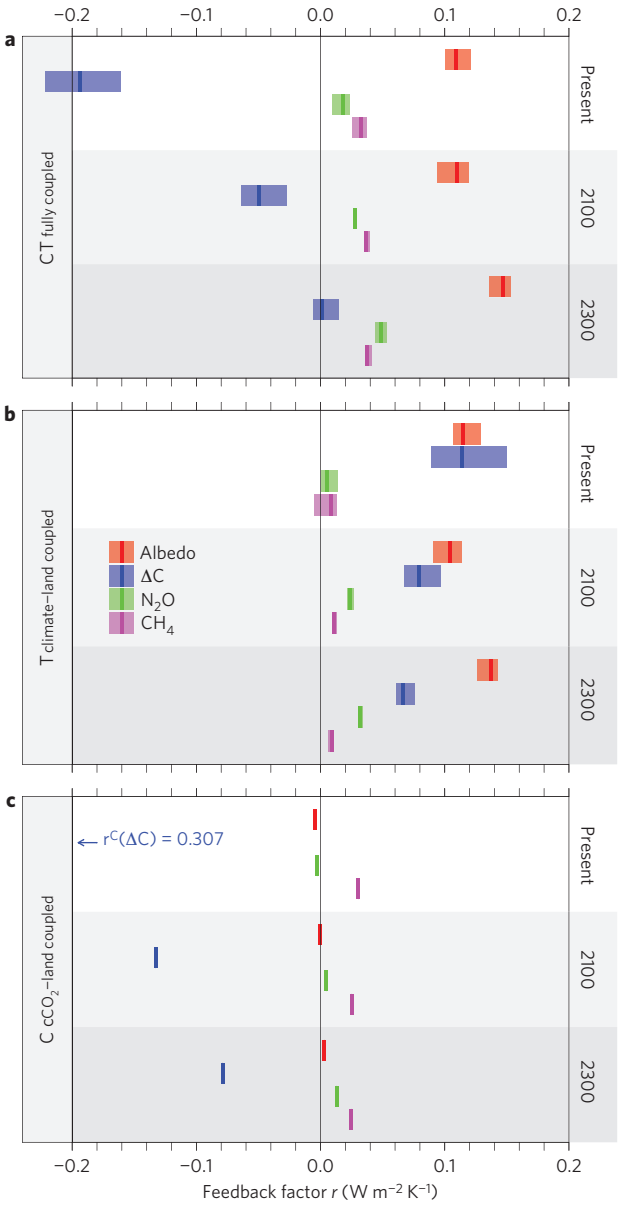

Figure 5 | Feedback factors. a–c, Feedback factors in fully coupled simulations (r_i^{CT}, with $i = \Delta C, eN_2O, eCH_4, \Delta$Albedo; **a**), in climate–land coupled simulations (r_i^T; **b**) and in cCO_2-land coupled simulations (r_i^C; **c**). Values are for present (mean of AD 2000–2010), 2100 (mean of 2095–2105) and 2300 (mean of 2290–2300). Rectangles represent minimum (left edge), maximum (right edge) and mean (middle line) of values derived from simulations with different climate change anomaly patterns from the five CMIP5 models applied. Results are from online RCP8.5 simulations. Feedback factors evaluated from RCP2.6 are given in Supplementary Fig. S21.

net feedback ($r_{\Delta C}^{CT}$) is small. The positive feedback from Albedo change remains effective and becomes the strongest positive land feedback in response to changes in climate by AD 2300. eN_2O and eCH_4 induce positive feedbacks in both climate–land and cCO_2–land coupled simulations, but their magnitude is smaller. Generally, non-ΔC feedbacks do not exhibit declining trends and increasingly affect the climate response to anthropogenic forcing in the long run. In addition, effects of C–N interactions, sensitivity of peatland C-storage and land-use change—features not represented in last-generation terrestrial biosphere models presented in the IPCC AR4 (ref. 5)—each tend to enhance the total land feedback r_{land} in our model on long timescales and under high radiative forcings as in RCP8.5 (see Supplementary Fig. S18).

Limiting the rise in cCO_2 and climate change (RCP2.6) maintains a regime where the negative feedback from cCO_2-fertilization remains effective and the total land feedback is broadly neutral (Supplementary Fig. S21). Results also illustrate how reducing Nr inputs limits the amplification of eN_2O under future climate and thus mitigates the positive associated feedback.

Climate sensitivity is conventionally defined as the temperature change in response to a doubling of cCO_2 (+2.9 °C in Bern3D-LPX). Here, we quantify the effective climate sensitivity including land biogeochemical and land Albedo feedbacks in response to sustained radiative forcing of 3.7 W m^{-2}, corresponding to $2 \times cCO_2$, but allowing cCO_2 to evolve interactively. Climate sensitivity is increased from 2.8 °C (control set-up) to 3.2–3.3 °C (+15–20%) when land C stock and Albedo feedbacks are included and to 3.4–3.5 °C (+22–27%) when also feedbacks from eN_2O and eCH_4 are simulated (see Supplementary Fig. S7). Compared with a conventionally defined climate sensitivity, which commonly includes feedbacks from terrestrial Albedo changes, this is an amplification of 16–21%. Earth system models representing only carbon cycle and Albedo feedbacks, including a number of CMIP5 models, may thus underestimate the potential of land-based processes to amplify climate change through positive feedbacks.

Feedback strengths are subject to relatively large uncertainties associated with the representation of processes governing the sensitivity of terrestrial GHG emissions to climate and cCO_2. Values of feedback factors reported here are at the lower end of the range previously reported[1,6,7] where multiple agent interactions have not been accounted for. In our simulations, feedback uncertainties introduced by disagreement about climate change patterns are ±17% (AD 2100). Processes not represented in LPX-Bern (for example, changes in biogenic volatile organic carbon emissions and wetland extent) have the potential to further revise the total land feedback towards more positive values.

By applying an Earth system model, representing terrestrial biogeochemical cycling explicitly and interactively, we establish a consistent link between small-scale processes, with altered substrate availability and environmental conditions affecting denitrification and methane production, to the large scale, with amplified eCH_4 and eN_2O inducing positive land–climate feedbacks in a high-emission/business-as-usual scenario for the twenty-first century. The land biosphere is shifted from a regime where negative feedbacks from higher cCO_2 compensate smaller positive feedbacks from eN_2O and eCH_4 today to a state where non-ΔC feedbacks exert an increasingly strong additional warming in the future. These results suggest that land ecosystem feedbacks in addition to those directly related to carbon storage should be included in the next generation of comprehensive Earth system models.

Methods

Terrestrial processes are simulated with the LPX-Bern 1.0 model (Land surface processes and exchanges, Bern version 1.0), which unifies representations for natural[13], agricultural[14,20] and peatland[15,17,18] coupled C and N (ref. 16) dynamics and predicts the release/uptake of CO_2, N_2O and CH_4. The model version applied here uses a vertically resolved soil hydrology/heat diffusion scheme as a previous LPX version[30], but does not include the comprehensive fire scheme of ref. 30.

To assess the historical budgets and project GHG emissions under RCP2.6 and RCP8.5, we apply LPX in offline mode, where climate and atmospheric CO_2 concentration are prescribed (simulations termed offline). For the feedback quantification, LPX is coupled to the Bern3D Earth system model of intermediate complexity and GHG emissions are prescribed, whereas atmospheric GHG concentrations, radiative forcing and climate change are calculated online (simulations termed online). Bern3D simulates three-dimensional dynamics of ocean heat and CO_2 uptake[28], ocean biogeochemistry, and includes a two-dimensional Earth surface energy balance[29].

In both set-ups, inputs prescribed to LPX are N-deposition[23], mineral N-fertilization[24], croplands, pastures and urban areas, fixed lateral extent of

peatland areas and seasonally inundated wetlands. The historical N-fertilization data set is extended to AD 2100 in consistency with the RCP scenarios[25,26] (see Supplementary Information for complete references of input data).

In offline mode, temperature, precipitation and cloud cover are prescribed from CRU TS 3.1 (ref. 21) for the historical period and from the CMIP5 outputs for AD 2005–2100. As input to LPX, we selected outputs from five CMIP5 models (HadGEM2-ES, MPI-ESM-LR, IPSL-CM5A-LR, MIROC-ESM, CCSM4) covering a wide range of uncertainty with respect to model climate sensitivity and polar amplification and providing required climate variables for the RCP2.6 and RCP8.5 simulations (total 32 experiments, see Supplementary Table S1). CMIP5 data were offset-corrected to match the CRU data at present (mean of AD 1996–2005). In online mode, a spatial pattern per unit temperature change, derived for each CMIP5 model, is scaled by the global mean temperature change (ΔT) simulated online by Bern3D. To assess uncertainties, all offline simulations are performed for each CMIP5 model; all online simulations are performed for each anomaly pattern.

N_2O emissions from rivers are modelled as a constant fraction (0.6%) of leached nitrate. This yields a flux of 0.65 Tg N_2O–N yr^{-1} in AD 1900, increasing to 0.8 Tg N_2O–N yr^{-1} in 2005 AD. Simulated terrestrial emissions of CO_2, N_2O and CH_4 are complemented with other sources not simulated by LPX and an additional flux to close the pre-industrial atmospheric budget (see Supplementary Fig. S6). For the historical period, we use data for N_2O emissions not simulated by LPX as presented in ref. 24, but extend records in consistency with the RCP scenarios[25,26]. To close the pre-industrial atmospheric budget, we use an oceanic source of 3.3 Tg N_2O–N yr^{-1} increasing by 3.3% until 2005 AD in line with changes in total reactive Nr in the surface ocean due to atmospheric deposition[31].

For prescribed non-LPX CH_4 emissions we use total anthropogenic CH_4 emissions from the RCP database as they do not include any sources explicitly simulated by LPX. The pre-industrial atmospheric budget, based on Southern Hemisphere records, is closed by a geological source of 38 Tg CH_4 yr^{-1}, held constant thereafter.

Atmospheric concentrations are calculated using a simplified atmospheric chemistry model[32] to simulate variations in the lifetime of GHGs and using prescribed emissions of other reactive gases from the RCP database (VOC, NO_x, CO). Ocean biogeochemistry operates in all online simulations and affects cCO_2, but interactive ocean N_2O emissions are neglected. The radiative forcing of all agents affected by variations of terrestrial GHG emissions are simulated online in Bern3D after ref. 32. Radiative forcing from other agents (aerosols, HFCs, CFCs) is prescribed from the RCP database.

Feedbacks are evaluated following the framework outlined for climate–carbon cycle feedbacks in ref. 1 and schematically illustrated in Fig. 1. External radiative forcings are acting on the system without being affected by the state of the system, for example GHG emissions from fossil-fuel combustion, anthropogenic land-use change, nitrogen fertilizer application and so on. These affect the Earth energy balance with a radiative forcing F. In the absence of any feedbacks from terrestrial GHG emissions and Albedo change, that is, the land model does not see any changes in climate or cCO_2, this would lead to an increase in global mean temperature ΔT^{ctrl}. Positive (negative) feedbacks from land (λ_{land}) amplify (attenuate) this response and lead to a higher (lower) temperature change ΔT^{i}:

$$F = \lambda_0 \cdot \Delta T^{\mathrm{ctrl}} \quad (1)$$

$$F = (\lambda_0 + \lambda^{\mathrm{i}}_{\mathrm{land}}) \cdot \Delta T^{\mathrm{i}} \quad (2)$$

λ_0 is the sum of all non-land feedbacks (black-body, sea ice-Albedo, lapse rate, water vapour feedbacks and so on). Here, land feedbacks summarize effects from all forcing agents: changes in terrestrial C storage (ΔC), eN_2O, eCH_4 and Albedo ($\lambda^{\mathrm{i}}_{\mathrm{land}} \approx \lambda^{\mathrm{i}}_{\Delta C} + \lambda^{\mathrm{i}}_{\mathrm{CH_4}} + \lambda^{\mathrm{i}}_{\mathrm{N_2O}} + \lambda^{\mathrm{i}}_{\mathrm{Albedo}}$). They can be evaluated with respect to their drivers in a climate–land coupled ($i = T$, Fig. 1), a cCO_2–land coupled ($i = C$) or a fully coupled simulation ($i = CT$) and are related as $\lambda^{\mathrm{CT}} \approx \lambda^{\mathrm{C}} + \lambda^{\mathrm{T}}$. We refer to feedback factors as $r = -\lambda$, so that positive feedbacks have positive values and vice versa.

Received 30 July 2012; accepted 1 March 2013; published online 14 April 2013

References

1. Gregory, J. M., Jones, C. D., Cadule, P. & Friedlingstein, P. Quantifying carbon cycle feedbacks. *J. Clim.* **22,** 5232–5250 (2009).
2. Canadell, J. G. *et al.* Contributions to accelerating atmospheric CO_2 growth from economic activity, carbon intensity, and efficiency of natural sinks. *Proc. Natl Acad. Sci. USA* **104,** 18866–18870 (2007).
3. Hirsch, A. *et al.* Inverse modelling estimates of the global nitrous oxide surface flux from 1998–2001. *Glob. Biogeochem. Cycles* **20,** GB1008 (2006).
4. Davidson, E. A. The contribution of manure and fertilizer nitrogen to atmospheric nitrous oxide since 1860. *Nature Geosci.* **2,** 659–662 (2009).
5. Denman, K. L. *et al.* in *IPCC Climate Change 2007: The Physical Science Basis* (eds Solomon, S. *et al.*) Ch. 7 (Cambridge Univ. Press, 2007).
6. Arneth, A. *et al.* Terrestrial biogeochemical feedbacks in the climate system. *Nature Geosci.* **3,** 525–532 (2010).
7. Xu-ri Prentice, I. C., Spahni, R. & Niu, H. S. Modelling terrestrial nitrous oxide emissions and implications for climate feedback. *New Phytol.* **2,** 472–88 (2012).
8. Van Groenigen, K. J., Osenberg, C. W. & Hungate, B. A. Increased soil emissions of potent greenhouse gases under increased atmospheric CO_2. *Nature* **475,** 214–216 (2011).
9. Khalil, M. A. K. & Rasmussen, R. A. Climate-induced feedbacks for the global cycles of methane and nitrous oxide. *Tellus B* **41B,** 554–559 (1989).
10. Torn, M. S. & Harte, J. Missing feedbacks, asymmetric uncertainties, and the underestimation of future warming. *Geophys. Res. Lett.* **33,** L10703 (2006).
11. Frank, D. C. *et al.* Ensemble reconstruction constraints on the global carbon cycle sensitivity to climate. *Nature* **463,** 527–530 (2010).
12. Knutti, R. & Hegerl, G. C. The equilibrium sensitivity of the Earth's temperature to radiation changes. *Nature Geosci.* **1,** 735–743 (2008).
13. Sitch, S. *et al.* Evaluation of ecosystem dynamics, plant geography and terrestrial carbon cycling in the LPJ dynamic global vegetation model. *Glob. Change Biol.* **9,** 161–185 (2003).
14. Strassmann, K. M., Joos, F. & Fischer, G. Simulating effects of land use changes on carbon fluxes: Past contributions to atmospheric CO_2 increases and future commitments due to losses of terrestrial sink capacity. *Tellus B* **60,** 583–603 (2008).
15. Wania, R., Ross, I. & Prentice, I. C. Integrating peatlands and permafrost into a dynamic global vegetation model: 2. Evaluation and sensitivity of vegetation and carbon cycle processes. *Glob. Biogeochem. Cycles* **23** (2009).
16. Xu-Ri, & Prentice, I. C. Terrestrial nitrogen cycle simulation with a dynamic global vegetation model. *Glob. Change Biol.* **14,** 1745–1764 (2008).
17. Spahni, R., Joos, F., Stocker, B. D., Steinacher, M. & Yu, Z. C. Transient simulations of the carbon and nitrogen dynamics in northern peatlands: from the Last Glacial Maximum to the twenty first century. *Clim. Past Discuss.* **8,** 5633–5685 (2012).
18. Zürcher, S., Spahni, R., Joos, F., Steinacher, M. & Fischer, H. Impact of an 8.2-kyr-like event on methane emissions in northern peatlands. *Biogeosci. Discuss.* **9,** 13243–13286 (2012).
19. Spahni, R. *et al.* Constraining global methane emissions and uptake by ecosystems. *Biogeosciences* **8,** 1643–1665 (2011).
20. Stocker, B. D., Strassmann, K. & Joos, F. Sensitivity of Holocene atmospheric CO_2 and the modern carbon budget to early human land use: Analyses with a process-based model. *Biogeosciences* **8,** 69–88 (2011).
21. Mitchell, T. D. & Jones, P. D. An improved method of constructing a database of monthly climate observations and associated high-resolution grids. *Int. J. Climatol.* **25,** 693–712 (2005).
22. MacFarling Meure, C. *et al.* Law Dome CO_2, CH_4 and N_2O ice core records extended to 2000 years BP. *Geophys. Res. Lett.* **33,** L14810 (2006).
23. Lamarque, J-F. *et al.* Global and regional evolution of short-lived radiatively-active gases and aerosols in the representative concentration pathways. *Climatic Change* **109,** 191–212 (2011).
24. Zaehle, S., Ciais, P., Friend, A. D. & Prieur, V. Carbon benefits of anthropogenic reactive nitrogen offset by nitrous oxide emissions. *Nature Geosci.* **4,** 601–605 (2011).
25. Van Vuuren, D. P. *et al.* RCP2.6: Exploring the possibility to keep global mean temperature increase below 2 °C. *Climatic Change* **109,** 95–116 (2011).
26. Riahi, K. *et al.* RCP 8.5-A scenario of comparatively high greenhouse gas emissions. *Climatic Change* **109,** 33–57 (2011).
27. De Klein, C. *et al.* in *IPCC Guidelines for National Greenhouse Gas Inventories* Vol. 4 (eds Eggleston, H., Buendia, L., Miwa, K., Ngara, T. & Tanabe, K.) Ch. 11 (IGES, 2006).
28. Müller, S. A., Joos, F., Edwards, N. R. & Stocker, T. F. Water mass distribution and ventilation timescales in a cost-efficient, three-dimensional ocean model. *J. Clim.* **19,** 5479–5499 (2006).
29. Ritz, S. P., Stocker, T. F. & Joos, F. A coupled dynamical ocean energy balance atmosphere model for paleoclimate studies. *J. Clim.* **24,** 349–375 (2011).
30. Prentice, I. C. *et al.* Modelling fire and the terrestrial carbon balance. *Glob. Biogeochem. Cycles* **25,** GB3005 (2011).
31. Suntharalingam, P. *et al.* Quantifying the impact of anthropogenic nitrogen deposition on oceanic nitrous oxide. *Geophys. Res. Lett.* **39,** L07605 (2012).
32. Joos, F. *et al.* Global warming feedbacks on terrestrial carbon uptake under the Intergovernmental Panel on Climate Change (IPCC) emission scenarios. *Glob. Biogeochem. Cycles* **15,** 891–907 (2001).
33. Langenfelds, R. *et al.* in *Baseline Atmospheric Program Australia* (eds Cainey, J., Derek, N. & Krummel, P.) 55–56 (Bureau of Meteorology and CSIRO Atmospheric Research, 2004).
34. Buizert, C. *et al.* Gas transport in firn: Multiple-tracer characterization and model intercomparison for NEEM, Northern Greenland. *Atmos. Chem. Phys.* **12,** 4259–4277 (2012).

Acknowledgements

We acknowledge K. Riahi for providing RCP8.5 data, J-F. Lamarque for providing N-deposition data, climate modelling centres participating in CMIP5 as listed in Supplementary Table S1 for providing climate input data, and C2SM at ETHZ for processing and sharing the CMIP5 data. We thank P. Friedlingstein and Th. Stocker for discussions and inputs. We appreciate support by the Swiss National Science Foundation through the National Centre of Competence in Research Climate (NCCR) and the grant to the division of Climate and Environmental Physics, and by the European Commission through the FP7 project CARBOCHANGE (grant no. 264879) and Past4Future (grant no. 243908).

Author contributions

B.D.S. and R.R. share equal contributions to this work. B.D.S. prepared the model set-up, conducted the offline simulations, compiled the figures and wrote the text. R.R. prepared and conducted the online simulations, and delivered inputs for the model set-up and results analysis. R.S. and M.S. contributed substantially to the LPX model development and the simulations. S.Z. and L.B. provided N-fertilization and N_2O input data and technical advice. X-R. contributed substantially to the LPX model development. I.C.P. and F.J. initiated the study, guided the concept and edited the manuscript text. F.J. organized funding for B.S., R.R., R.S. and M.S.

Additional information

Supplementary information is available in the online version of the paper. Reprints and permissions information is available online at www.nature.com/reprints. Correspondence and requests for materials should be addressed to B.D.S.

Competing financial interests

The authors declare no competing financial interests.